

Submitted to ApJ June 2, 2005; accepted August 1, 2005

Kelu-1 is a Binary L Dwarf: First Brown Dwarf Science from Laser Guide Star Adaptive Optics

Michael C. Liu¹

Institute for Astronomy, University of Hawai‘i, 2680 Woodlawn Drive, Honolulu, HI 96822

mliu@ifa.hawaii.edu

and

Sandy K. Leggett

United Kingdom Infrared Telescope, Joint Astronomy Centre, 660 North A’ohoku Place, Hilo, HI 96720

skl@jach.hawaii.edu

ABSTRACT

We present near-infrared (1–2.4 μm) imaging of the L dwarf Kelu-1 obtained with the Keck sodium laser guide star adaptive optics (LGS AO) system as part of a high angular resolution survey for substellar binaries. Kelu-1 was one of the first free-floating L dwarfs identified, and the origin of its overluminosity compared to objects of similar spectral type has been a long-standing question. Our images clearly resolve Kelu-1 into a 0.29'' (5.4 AU) binary with near-infrared flux ratios of ≈ 0.5 mags. A previous non-detection of binarity by *Hubble Space Telescope* demonstrates that the system is a true physical pair and that its projected orbital motion has been significant over the last 7 years. Binarity explains the properties of Kelu-1 that were previously noted to be anomalous compared to other early-L dwarfs. We estimate spectral types of L1.5–L3 and L3–L4.5 for the two components, giving model-derived masses of 0.05–0.07 M_\odot and 0.045–0.065 M_\odot for an estimated age of 0.3–0.8 Gyr. More distant companions are not detected to a limit of $\approx 5\text{--}9 M_{Jup}$. The presence of Li 6708 Å absorption indicates that both components are substellar, but the weakness of this feature relative to other L dwarfs can be explained if only Kelu-1B is Li-bearing. Determining whether both or only one of the components possesses lithium could constrain the age of Kelu-1 (and other Li-bearing L binaries) with higher precision than is possible for most ultracool field objects. These results are the first LGS AO observations of brown dwarfs and demonstrate the potential of this new instrumental capability for substellar astronomy.

¹Alfred P. Sloan Research Fellow

Subject headings: binaries: general, close — stars: brown dwarfs — infrared: stars — techniques: high angular resolution

1. Introduction

Over a decade since they were first discovered, brown dwarfs are now being found in abundance from optical and infrared (IR) imaging surveys (e.g. Kirkpatrick et al. 1999; Delfosse et al. 1999; Hawley et al. 2002). While many hundreds of substellar objects have been identified, their physical properties and their origin(s) continue to be active areas of inquiry. Multiplicity is a key pathway towards understanding these issues. The substellar binary frequency, separation distribution, and mass ratio distribution can constrain the formation mechanisms for brown dwarfs (e.g. Bate et al. 2002). Substellar binaries also provide systems with a common age and metallicity, which can aid interpretation of physical properties such as colors and spectra. Finally, dynamical mass determinations for substellar binaries are sorely needed to test the theoretical models over a wide range of parameter space. To date, only two ultracool binaries have such measurements (GL 569Bab: Lane et al. 2001; Zapatero Osorio et al. 2004; 2MASSW J0746425+2000321AB: Bouy et al. 2004).

Previous imaging surveys of nearby ultracool objects, primarily by *Hubble Space Telescope* (*HST*) at optical wavelengths (Koerner et al. 1999; Reid et al. 2001; Close et al. 2003; Bouy et al. 2003; Gizis et al. 2003), find that substellar binaries typically have $\lesssim 0.5''$ separations and that smaller separations are more common than larger ones — therefore, high angular resolution is a major premium for imaging studies. The spectral energy distributions of brown dwarfs peak in the near-IR and hence these wavelengths are advantageous for detection and characterization of substellar binaries, especially for cooler objects. Coincidentally, ground-based adaptive optics (AO) systems are most easily developed at these wavelengths. Since the largest ground-based telescopes have $\approx 4 \times$ larger apertures than *HST*, and hence the potential for $\approx 4 \times$ higher angular resolution, near-IR AO observations are an appealing capability for examining substellar multiplicity. However, natural guide star AO observations are hampered by the need for a bright star for wavefront sensing. In particular, the ultracool L and T dwarfs are too faint for natural guide star AO, and thus AO observations of these objects have largely been restricted to the rare objects found as companions to bright stars (Liu et al. 2002; Potter et al. 2002; Freed et al. 2003; McCaughrean et al. 2004; Metchev & Hillenbrand 2004; Burgasser et al. 2005)

Laser guide star (LGS) AO provides a powerful new tool for high angular resolution imaging and spatially resolved spectroscopy of substellar binaries. Through resonant scattering off the sodium layer at ~ 90 km altitude in the Earth's atmosphere, sodium LGS systems create an artificial star bright enough to serve as a wavefront reference for AO correction (Foy & Labeyrie 1985; Thompson & Gardner 1987; Happer et al. 1994). Thus, most of the sky can be made accessible to near diffraction-limited IR imaging from the largest existing telescopes. Also, ground-based telescopes can serve as enduring long-term platforms for high resolution imaging, which are needed for dynamical mass determinations of substellar binaries.

Here we present the first brown dwarf science obtained with LGS AO, observations of the ultracool dwarf Kelu-1 (Ruiz et al. 1997). Discovered in a photographic proper motion survey, this was one of the first free-floating L dwarfs identified. Given its low effective temperature, the presence of Li absorption in its spectrum clearly demonstrated its substellar nature, based on the lithium test (Rebolo et al. 1992; Basri 1998). Kelu-1 has served as a key object in spectral classification schemes for L dwarfs (Kirkpatrick et al. 1999; Martín et al. 1999b; Geballe et al. 2002). It has been assigned a spectral type of L2 by Kirkpatrick et al. based on optical spectra and L3±1 by Geballe et al. based on optical and IR spectra.

Once its parallax was measured (Dahn et al. 2000), Kelu-1 appeared to be overluminous compared to other early-L dwarfs (Martín et al. 1999b; Leggett et al. 2002), attributed either to an unusually young (<0.1 Gyr) age or an unresolved close companion. As the number of parallax measurements, and hence absolute magnitudes, for ultracool dwarfs have grown, Kelu-1’s apparent overluminosity has persisted (Dahn et al. 2002; Vrba et al. 2004). Based on all the observations to date, Golimowski et al. (2004a) argued that unresolved binarity remains the most compelling explanation, given the very young age (~ 10 Myr) otherwise needed to explain Kelu-1’s variance with other early-L dwarfs in the solar neighborhood. (Note that such a young age would imply a model-derived mass of only $\sim 12 M_{Jup}$ for Kelu-1, comparable to radial velocity planets found around other nearby stars.)

However, attempts to detect a companion to Kelu-1 have thus far been unsuccessful. *HST* near-IR imaging failed to identify any companion as close as 0.1'' (1.9 AU; Martín et al. 1999a), apparently favoring the youthful interpretation of Kelu-1. Clarke et al. (2002) detected photometric variability from Kelu-1 with a period of about 1.8 hrs, which they suggested might arise from ellipsoidal variations due to a very close substellar companion, but radial velocity monitoring data rule out this possibility (Clarke et al. 2003). Kelu-1’s status as one of the archetypical L dwarfs provides a compelling reason to understand the origin of its overluminosity. Therefore, we targeted this object with the new LGS AO system on the Keck II Telescope as part of a high angular resolution survey for substellar binaries.

2. Observations

We observed Kelu-1 on 2005 May 1 UT using the newly commissioned sodium LGS AO system (Bouchez et al. 2004; Wizinowich et al. 2004) of the 10-meter Keck II Telescope on Mauna Kea, Hawaii. We used the facility IR camera NIRC2 and the J (1.25 μm), H (1.64 μm), and K' (2.12 μm) filters from the Mauna Kea Observatories (MKO) filter consortium (Simons & Tokunaga 2002; Tokunaga et al. 2002). Conditions were photometric with excellent seeing conditions during the night, better than 0.6'' in the optical as reported by the neighboring Keck I Telescope. The total setup time for the telescope to slew to Kelu-1 and for the LGS AO system to be fully operational was 10 minutes.

Kelu-1 was observed as it transited, at an airmass of 1.4. The LGS brightness, as measured by the flux incident on the AO wavefront sensor, was equivalent to a $V \approx 10.1$ mag star. The LGS provided the wavefront reference source for AO correction, with the exception of tip-tilt motion. This was sensed using an $R = 14.3$ mag star from the USNO-B catalog (Monet et al. 2003) located $27''$ away from Kelu-1. The LGS AO-corrected images have full widths at half maximum (FWHM) of $0.08'', 0.07'',$ and $0.06''$ at JHK' , respectively, with corresponding Strehl ratios of 0.03, 0.08, and 0.20. The RMS variations in the FWHM and Strehl ratios between individual images were about 6% and 15%, respectively.

We obtained a series of six images in each filter, dithering the telescope by a few arcseconds between each pair of images. The total on-source integration time per filter was 3 minutes. The sodium laser beam was steered with each dither such that the LGS remained on Kelu-1 for all the images. Kelu-1 was easily resolved into a binary system in all our data. The images were reduced in a standard fashion. We constructed flat fields from the differences of images of the telescope dome interior with and without lamp illumination. Then we created a master sky frame from the median average of the bias-subtracted, flat-fielded images and subtracted it from the individual images. Images were registered and stacked to form a final mosaic (Figure 1).

To measure the flux ratios and relative positions of the two components, we employed two approaches: (1) aperture photometry and (2) fitting of an analytic model for the point spread function (PSF). For aperture photometry, we used small circular apertures ($\approx 1\text{-}3 \times \text{FWHM}$ diameter) centered on each component to determine the flux ratio, measuring both the direct images and those created by removing the light from the other component via rotating and subtracting the images. For the case of the analytic fit, the PSF was modeled as two gaussian components, a narrow component for the PSF core and the broad component for the PSF halo. All the individual images were fit separately. The two methods agreed very well, as expected given the fact that the binary is well-resolved and has a modest flux ratio. We adopted the averages of all the measurements of individual images as the final results and the standard deviations as the errors. For the separation and position angle, no systematic offset was seen between the JHK' dataset, and thus we combined the measurements from all three filters.

Table 1 presents the resulting flux ratios and astrometry from the Keck LGS AO images. Table 2 reports the calculated IR colors and magnitudes of the individual components. To derive these from the observed flux ratios, we used the integrated IR magnitudes reported in Leggett et al. (2002) and Knapp et al. (2004). Any error due to photometric variability is likely to be negligible. Kelu-1 shows variability at optical wavelengths with 1–2% amplitude (Clarke et al. 2002, 2003); near-IR variability at this level would not impact our measurements. Similarly, near-IR monitoring of a small number of L dwarfs finds little variability (Bailer-Jones & Lamm 2003; Bailer-Jones 2002). Absolute magnitudes were determined using the parallactic distance of 18.7 ± 0.7 pc (Dahn et al. 2002).¹

¹As described in § 3, the projected separation of the binary has changed from 1998 to 2005. Therefore, the

Our NIRC2 J and H -band photometry used the same MKO filters as Leggett et al. (2002) and Knapp et al. (2004) and hence computing magnitudes for the individual components from our measured flux ratios is straight-forward. However, our NIRC2 data were obtained with the MKO K' -band ($2.12\text{ }\mu\text{m}$) filter, in order to minimize the thermal background from the sky + AO system, whereas the published photometry used the MKO K -band ($2.20\text{ }\mu\text{m}$) filter. The measured near-IR colors of L dwarfs are sensitive to the specific choice of filters due to the highly structured spectra of these very cool objects. Following Stephens & Leggett (2004), we use synthetic photometry to determine the $(K'-K)$ color as a function of spectral type for L1 to T9 dwarfs:

$$(K' - K)_{MKO} = -0.007526 + 0.029263 \times (SpT) - 0.0039505 \times (SpT)^2 + 0.00010163 \times (SpT)^3 \quad (1)$$

where $SpT = 0$ for L0 dwarfs, $=1$ for L1 dwarfs, $=10$ for T0 dwarfs, etc. For the range of spectral types relevant to Kelu-1A and B (see below), the color term is 0.04–0.05 mags. The RMS scatter about the polynomial fit is 0.05 mags, which we add in quadrature when computing the K -band photometric errors.

Aside from Kelu-1, the only other source detected in our images was 2MASS J1305400–2541122, whose 2MASS JHK_S colors (Bessell & Brett 1988) and change in position relative to Kelu-1 between our 2005 images and the 1998 2MASS data are consistent with a late-type background giant. For objects at $\gtrsim 1''$ from Kelu-1, the final mosaics reached a point source detection limit of 20.4, 20.5, and 19.9 mags at JHK' , respectively, out to a separation of $3''$. Based on the models of Baraffe et al. (2003) and an assumed age of 0.3–0.8 Gyr (see § 4), these limits correspond to about 5–9 M_{Jup} companions around Kelu-1.

3. Results

The companion detected in our images has exceptionally red IR colors, characteristic of L dwarfs. Also, the companion has redder colors than the primary, indicating a lower temperature. While our single epoch of Keck data by itself cannot prove the two objects are physically associated, it is highly unlikely the companion is an unrelated background source. For instance, in a 1 deg^2 region around Kelu-1, the 2MASS catalog has only 2 other well-detected ($S/N > 10$) sources of comparable or fainter IR magnitudes and comparable or redder IR colors. The odds of at least one such a source falling within our 100 arcsec^2 NIRC2 images are 1.5×10^{-5} .

photocenter of the combined system has been moving relative to the center of mass (because each component's emitted flux is not linearly related to its mass). In principle, such motion could have affected the parallax and proper motion determined by Dahn et al. (2002). They obtained 30 observations over 3.3 years, during which time the projected separation of the A and B components may have changed by $\sim 0.15''$. This concern is slightly abated by comparison with the preliminary parallax reported by Dahn et al. (2000): their parallax based on 1.3 years worth of data is consistent with the 3.3-year dataset. (However, the proper motion of the Dahn et al. measurements are somewhat discrepant with each other and with the results reported by Ruiz et al. 1997, which were based on two photographic observations taken 14 years apart.) Once the orbit of the system is more fully determined, the relative motion of the photocenter can be accounted for in the astrometry calculations.

Proof that the binary is a physically bound pair comes from the *HST*/NICMOS near-IR imaging obtained by Martín et al. (1999a) in August 1998. They did not detect any companion to Kelu-1 as close as 0.1'' separation (19 AU). Retrieving their images from the HST Archive, we find no other sources within 5'' of Kelu-1. Given Kelu-1's proper motion ($\mu = 0.285''/\text{yr}$ and $0.35''/\text{yr}$, PA = 272° and 265° , as reported by Dahn et al. 2002 and Ruiz et al. 1997, respectively), the source we identify as Kelu-1B would be expected to appear about 2'' west of Kelu-1A in the NICMOS images if the two objects were not physically associated. Thus, the *non-detection* of Kelu-1B in the earlier *HST* imaging demonstrates that the system is a physical pair (see § 4.4 for further discussion).

To infer spectral types, we compared the measured *JHK* colors and absolute magnitudes of the two components to late-M and L dwarfs with known distances (Figure 2). We assume that the components are themselves single, and not unresolved binaries, an assumption that is largely consistent with the observational constraints described below. For the comparison field sample, we used the nearby ultracool dwarf sample presented in Leggett et al. (2002), Knapp et al. (2004), and Golimowski et al. (2004a), which have photometry on the MKO system and spectral types using the Geballe et al. (2002) scheme. (We exclude the L2.5 dwarf SDSS 1435-0043, whose parallax is measured only with S/N=3, compared to the S/N \gtrsim 10 measurements typical for the rest of the sample.) We add objects from the McLean et al. (2003) spectral library with known parallaxes, converting the magnitudes and spectral types to the Geballe and MKO systems.

In general, *JHK* colors alone are not well-suited for spectral typing of L dwarfs, since there is a large color scatter at a given type (e.g. Kirkpatrick et al. 2000; Leggett et al. 2002). The *JHK* colors of Kelu-1A and 1B are consistent with L1–L5 and L3–L9 spectral types. However, the integrated-light spectral type of L3 indicates that component A cannot be later-type than L3. Furthermore, given this constraint on Kelu-1A, the modest IR flux ratios (0.4–0.7 mags) mean that component B cannot be a very late-L dwarf, since otherwise its magnitudes and luminosity would be too faint. If Kelu-1A is an L3 dwarf, Kelu-1B could be no later than L6, based on the flux ratios between L3 dwarfs and later-type L dwarfs shown in Figure 2.² Thus, the resolved *JHK* colors, the published integrated-light spectral type, and the IR flux ratios constrain the spectral types to be L1–L3 and L3–L6 for the two components.

Slightly more refined spectral type estimates come from comparing with the absolute IR magnitudes of field objects. IR magnitudes are well-correlated with spectral type, except for the late-L's and early-T's (Dahn et al. 2002; Vrba et al. 2004). We fit an unweighted 3rd-order polynomial to the spectral type as a function of absolute magnitude for field objects from M6 to L7.5. We

²When using the observed *JHK* flux ratios to estimate the spectral type of Kelu-1B relative to Kelu-1A, it may appear that we have implicitly assumed that the Kelu-1 system has a similar age to the comparison field sample. However, this is not the case. We have only assumed that the flux ratios of different type L dwarfs do not change, e.g., that the flux ratio of an early-L dwarf compared to a late-L dwarf is independent of age. For a given conversion from spectral type to T_{eff} , this is equivalent to assuming that the ratio of the two radii is constant with age; this constancy is demonstrated by the fact that the isochrones in Figure 4 are nearly parallel.

exclude known binaries from the fit.³ The final resulting spectral type estimates for the two Kelu-1 components are L1.5–L3 and L3–L4.5, with the independent JHK datasets providing consistent results. The quoted range in spectral type arises from the RMS scatter of the polynomial fit to the data.⁴ With these final spectral types, we compute the bolometric luminosities (L_{bol}) of each component, using the K -band bolometric corrections from Golimowski et al. (2004a), and tabulate the results in Table 2.

4. Discussion: Physical Properties in Light of the Binarity

4.1. Magnitudes, Colors, and T_{eff}

The long-noted overluminosity of Kelu-1 relative to other early L dwarfs is clearly explained by its binarity. The binarity also helps to explain its position in IR color-magnitude diagrams (CMDs; Figure 2). In integrated light, Kelu-1 appears to be unusually red in $J - K$ compared to its absolute magnitude, which led Dahn et al. (2002) to speculate on a possible connection between its redness and its photometric variability (Clarke et al. 2002) and/or large $v \sin i$ (Basri et al. 2000). However, Figure 2 shows that the resolved photometry of the A and B components is consistent with the location of other apparently single L dwarfs. (Interestingly, the location of Kelu-1B in the CMDs is similar to known mid-L binaries, perhaps suggesting that it is an unresolved system.)

Figure 2 also shows that nearly all the L dwarf binaries are the reddest objects in $J - K$ at a given magnitude. This is expected: most known substellar binaries have IR flux ratios close to unity, and since later-type L dwarfs are redder, unresolved L dwarf binaries should occupy a CMD position which is redder than other objects at the same absolute magnitude. Likewise, the most luminous sources at a given IR color are the most likely candidates for binarity.⁵ Therefore, some of the scatter in the IR CMD must arise from unrecognized binarity. Other effects can also introduce significant scatter, such as a large age spread in the local population and the effect of condensate clouds on the IR fluxes (Marley et al. 2002). A complete binary census of the nearby L dwarfs

³The close binaries plotted in Figure 2 are LHS 2397a (M8 primary; Freed et al. 2003), 2MASSW 0746+2000 (L1 primary; Reid et al. 2001), GJ 1001BC (L4 primary; Golimowski et al. 2004b), DENIS-P J0204.4–1150 (L5.5 primary; Koerner et al. 1999), DENIS-P 1228.2–1547 (L6 primary; Martín et al. 1999a), 2MASSs 0850+1057 (L6 primary; Reid et al. 2001), and GL 337CD (L9.5 in combined-light; Burgasser et al. 2005).

⁴Here we have assumed that the age of Kelu-1 is not very different than the comparison field sample, since we are comparing absolute magnitudes. However, as discussed in § 4, Kelu-1 is somewhat younger than the field population but not enough to significantly affect the spectral type estimate (e.g., see the isochrones in Figure 4).

⁵The clear exception in Figure 2 is GL 337CD, which has an L9.5 integrated-light spectral type on the Geballe et al. (2002) scheme (as computed by us using the spectrum from McLean et al. 2003). This binary (Burgasser et al. 2005) has an unusually blue $J - K$ integrated-light color given its spectral type and IR magnitude. These properties could be explained if the binary is composed of a late-L dwarf and an early-T dwarf, given the comparable J -band magnitudes but greatly different IR colors of such objects.

would be valuable to understand the relative significance of these effects.

Binarity also explains the apparently discrepant effective temperature (T_{eff}) of Kelu-1. Golimowski et al. (2004a) found that Kelu-1’s T_{eff} of 2300 K is ≈ 400 K hotter than the other L3 dwarfs in their sample (accounting for the younger age of Kelu-1 relative to the rest of their sample). To estimate the T_{eff} of the individual components, we can use the measured K -band flux ratio to estimate the bolometric luminosity ratios, since Golimowski et al. find that the K -band bolometric corrections are nearly constant for early to mid-L dwarfs. The individual T_{eff} ’s are then given simply by scaling from the T_{eff} originally computed, e.g., $T_{\text{eff},A} = (L_A/L_{A+B})^{1/4} \times (T_{\text{eff},A+B})$, where L_A is the bolometric luminosity for component A and L_{A+B} for the combined system. Thus we estimate $T_{\text{eff},A} \approx 2020$ K and $T_{\text{eff},B} \approx 1840$ K, in accord with other L2–L3 and L4 dwarfs, respectively, studied by Golimowski et al.

4.2. Lithium: Substellar Status and Age Determination

Lithium is fully depleted over the lifetime of low-mass stars and high mass ($\gtrsim 0.065 M_{\odot}$) brown dwarfs (Rebolo et al. 1992; Chabrier et al. 1996; Ushomirsky et al. 1998). The presence of Li absorption in L dwarfs ($T_{\text{eff}} \approx 1600 - 2300$ K; Golimowski et al. 2004a) is a clear indicator of substellar status, since objects with $T_{\text{eff}} \lesssim 2700$ K which show lithium must be below the lithium-burning limit of $0.065 M_{\odot}$ (Basri 1998). Kelu-1 shows Li I 6708 Å absorption in its spectrum, with an equivalent width (EW) of about 1 Å (Ruiz et al. 1997; Kirkpatrick et al. 1999). However, the binarity of Kelu-1 raises the question of whether only the lower-mass component possesses Li, with the higher-mass component having destroyed it.

A simple estimate shows that Kelu-1B could plausibly be the sole Li-bearing component of the binary. The flux ratios of L1–L2.5 dwarfs (i.e., Kelu-1A) to L3–L4.5 dwarfs (i.e., Kelu-1B) are expected to be ≈ 0.5 – 2.0 mags at optical wavelengths near the Li 6708 Å line, based on absolute magnitudes from Dahn et al. (2002) and Hawley et al. (2002). If the Li absorption line resides solely with Kelu-1B, the broad-band optical flux ratios allow us to estimate the dilution due to the Kelu-1A and thus the true line strength. (Here we ignore the detailed differences between the optical continua of the early and mid-L dwarfs.) For optical flux ratios of 0.5– 2.0 mags, Kelu-1B would have to have $\text{EW}(\text{Li}) \approx 2.5$ – 7 Å to produce the observed combined-light $\text{EW}(\text{Li})$. Such an $\text{EW}(\text{Li})$ is consistent with other L3–L4 dwarfs (Kirkpatrick et al. 2000). Indeed, the combined-light $\text{EW}(\text{Li})$ of Kelu-1 is relatively low compared to other early-L’s, originally suggestive of partial depletion (Basri et al. 1998; Kirkpatrick et al. 2000). This apparent deficiency is naturally explained by Kelu-1B being the sole Li-bearing component.

However, given Kelu-1B’s estimated spectral type of L3–L4.5 ($T_{\text{eff}} \approx 1750$ – 1950 K; Golimowski et al. 2004a), the fact that at least it possesses lithium shows that *both* components of Kelu-1 are substellar, regardless of whether Kelu-1A has Li. This is shown in Figure 3, which compares the derived L_{bol} ’s for the two components against models for lithium depletion from Burrows et al.

(1997) and Baraffe et al. (1998). The models indicate that the presence of lithium gives an upper age of 0.8 Gyr for the system. (We assume that depletion of the initial abundance by a factor of 100 demarcates the detection limit for lithium absorption. Since depletion occurs quickly, the derived upper age does not depend strongly on the adopted depletion factor.) This upper age of 0.8 Gyr results in upper mass estimates of $0.065\text{--}0.07 M_{\odot}$ and $0.06\text{--}0.065 M_{\odot}$ for components A and B, respectively. The stellar/substellar boundaries in the Burrows and Baraffe et al. models are 0.075 and $0.072 M_{\odot}$, respectively, and therefore we conclude that Kelu-1A is also a substellar object.

Spatially resolved high resolution optical spectroscopy of the two components would refine the age estimate for Kelu-1 to better than is generally possible for field objects. Early-L dwarfs with ages of $\gtrsim 0.6$ Gyr are massive enough to deplete their lithium (Figure 3). Thus, if Kelu-1A has no lithium but Kelu-1B does, the estimated age of the system would be $\approx 0.6\text{--}0.8$ Gyr. Likewise, if both components possess lithium, the binary’s estimated age would be $\lesssim 0.6$ Gyr.

Exploiting the differing Li depletion timescales for objects of different masses offers an appealing method for age-dating L dwarf binaries. This approach is analogous to the lithium depletion boundary technique used to determine ages for young open clusters (e.g. Basri et al. 1996). Age estimates are needed in combination with dynamical masses to test theoretical evolutionary models, but substellar binaries in the field have poorly constrained ages.⁶ Li-bearing L dwarf binaries are uncommon, with 6 such systems of the 21 known L dwarf binaries (see compilation in Close et al. 2003, with the addition of GJ 1001BC from Golimowski et al. 2004b and Kelu-1AB from this work). Among these 6 Li-bearing systems, 4 of them have separations larger than $0.2''$, making them amenable to resolved optical spectroscopy with very good (e.g., tip-tilt corrected) angular resolution: DENIS-P J1228.2–1547 (Martín et al. 1999a; Tinney et al. 1997), 2MASSW J1239+5515 (Bouy et al. 2003; Gizis et al. 2003; Kirkpatrick et al. 2000), 2MASSW J1146+2230 (Reid et al. 2001; Kirkpatrick et al. 1999), and Kelu-1. Measuring different lithium contents for their individual components could provide a sample of binaries with age estimates better than possible for typical substellar binaries.⁷

⁶For substellar binaries around main-sequence stars (see compilation in Burgasser et al. 2005), somewhat better constraints are possible based on indirect age indicators for the primary stars, such as stellar activity and/or kinematics (e.g. Lachaume et al. 1999).

⁷The other two known Li-bearing L dwarf binaries are the $0.06''$ system 2MASSW 1112+3548 (Bouy et al. 2003; Kirkpatrick et al. 2000) and the $0.16''$ system 2MASSs J0850+1057 (Reid et al. 2001; Kirkpatrick et al. 1999). Note that 0850+10 may be composed of an L dwarf primary and a T dwarf secondary, in which case it may not be suitable for this age-dating approach since atomic lithium converts to molecular form for T dwarfs (Burrows & Sharp 1999). This method could also be applied to low-mass binaries composed of a late-M dwarf and an L dwarf. However, since M dwarfs deplete lithium much faster than L dwarfs, the resulting age constraint would have a much larger range.

4.3. Estimated Age Range and Component Masses

In order to estimate the masses of the components, we must first estimate the age of the system. The Li detection discussed above leads to an upper age limit of 0.8 Gyr. The lower age is less well-constrained but cannot be arbitrarily young: if the assumed age is too small, then given the inferred T_{eff} , the observed magnitudes and L_{bol} 's would be too bright compared to model predictions (see below). From optical spectroscopy of gravity-sensitive features, McGovern et al. (2004) infer that Kelu-1 is older than the L2 dwarf G196-3B, whose age is estimated to be 0.02–0.3 Gyr based on the properties of its M dwarf primary star G196-3 (Rebolo et al. 1998). Hence, we initially adopt a lower bound of 0.1 Gyr for the Kelu-1 system.

As a first estimate of the masses, we use the measured L_{bol} 's with the adopted 0.1–0.8 Gyr age and compare to theoretical models (Figure 3). The resulting mass estimates are 0.025–0.07 M_{\odot} and 0.02–0.065 M_{\odot} for components A and B, respectively. The age of the system dominates the uncertainties in the masses, since the iso-mass lines in Figure 3 are mostly vertical. Note that the model-inferred mass ratio of the system is relatively independent of the exact age, with component A expected to be about 10–20% more massive than component B.

A more refined estimate of the masses is possible by including the effective temperatures as additional constraints. We use our spectral type estimates of L1.5–L3 and L3–L4.5 to derive T_{eff} for the two components, based on the Golimowski et al. (2004a) scale. Figure 4 shows the resulting mass estimates using the L_{bol} , age, and T_{eff} information, under the assumption that the conversion from spectral type to T_{eff} is age-independent for $\gtrsim 0.1$ Gyr.⁸ The lower age range of 0.1 Gyr appears to set a lower mass estimate of 0.03 M_{\odot} for Kelu-1B, depending on the choice of models. However, if the system were as young as 0.1 Gyr, Kelu-1A would be too faint for an object of type L3 or earlier ($T_{\text{eff}} \gtrsim 1950$ K) compared to the models. Thus, the T_{eff} and L_{bol} constraints from Kelu-1A in Figure 4 lead to a revised lower age limit of ≈ 0.3 –0.4 Gyr, depending on the choice of models, and thereby giving lower mass estimates of 0.05 M_{\odot} for A and 0.045 M_{\odot} for B (Figure 3). These mass estimates are slightly more restrictive than those derived without using the effective temperatures.

4.4. Orbital Motion

The joint information provided by the *HST* non-detection and our Keck detection can provide some crude insight into the binary's orbit, from examining the chances that the *HST* observation occurred at a time when the binary's projected separation was much smaller than the current value.

⁸The Golimowski et al. scale is derived from field objects, most of which are probably $\approx 10\times$ older than Kelu-1AB. Theoretical models predict that brown dwarf radii change by no more than 30% from 0.1–10 Gyr (Burrows et al. 2001). The concomitant change in surface gravity is 0.2 dex, a small amount. On the other hand, potentially important factors such as variations in dust content and rotation are not well-characterized and may lead to greater age-sensitivity in the relation between spectral type and T_{eff} than expected from surface gravity differences alone.

Brown (2004) has computed the probability of discovering a companion from a single observation in the situation where the object cannot be detected too close to the primary, assuming a random orbital phase and longitude of periastron. This probability depends on the companion orbital parameters and the minimum radius for detection (the “obscuration radius”). Assuming that Kelu-1’s orbit is circular and that the 2005 position represents the extreme projected separation (i.e., the semi-major axis), the ratio of the semi-major axis to the *HST* obscuration radius ($\approx 0.1''$) is a factor of ≈ 3 . Brown (2004) show that the probability of not detecting such a companion in a single observation is about 5%, assuming a modest (< 0.35) orbital eccentricity. Thus under these assumptions, the *HST* non-detection was improbable but only at the $\approx 2\sigma$ level. However, for a semi-major axis of $0.7''$, there is only a 1% chance that *HST* would not have seen the companion. Therefore, the semi-major axis of Kelu-1B is unlikely to be greater than $\sim 2 \times$ its current separation.

Basically, the true semi-major axis of the Kelu-1AB system is unlikely to be much larger than the current projected separation, or else *HST* would have almost certainly resolved the binary. Note that the likelihood of the *HST* non-detection rises if the orbit is eccentric and the semi-major axis is closer to the obscuration radius, i.e., smaller than the current separation (Brown 2004). Also if the orbit is circular, the *HST* non-detection and Keck detection indicate that the orbit must be close to edge-on, with a lower limit of $\approx 70^\circ$ for the inclination. In this situation, the expected amplitude of the radial velocity reflex motion would be $\approx 2 \text{ km s}^{-1}$, perhaps detectable with current near-IR spectrographs provided multi-year stability can be achieved.

We can make a rough estimate of the orbital period, assuming that the true semi-major axis is not very different than the observed projected separation. For a 5.4 AU semi-major axis, the estimated total system mass of $\approx 0.12 M_\odot$ ($0.095\text{--}0.135 M_\odot$) gives an expected orbital period of 37 years (34–41 years). More generally, Torres (1999) show that $\approx 85\%$ of randomly oriented orbits have a true semi-major axis of 0.5–2.0× the projected separation, corresponding to periods of $\approx 15\text{--}105$ yr for Kelu-1AB.

5. Summary

Keck LGS AO imaging has revealed the binary nature of the nearby L dwarf Kelu-1. Non-detection by *HST* in 1998 demonstrates that the system is a true physical pair, and that the orbital motion over the last 7 years has been significant. The non-detection also indicates that the true semi-major axis of the system is unlikely to be much larger than the currently observed $0.29''$ separation, or else the *HST* non-detection would have been highly improbable.

The binarity of Kelu-1 explains the long-noted anomalies of this object relative to other early-L dwarfs, namely its overluminosity, its very red IR colors, and its unusually large inferred T_{eff} . Its low Li absorption line strength relative to other early-L dwarfs may also be explained by binarity — Kelu-1B could be the sole component possessing lithium, with the light from the non-Li-bearing Kelu-1A leading to a relatively weak absorption line in the integrated-light spectrum. Comparing

the resolved *JHK* colors and magnitudes, and the integrated-light spectral type to other field objects leads to spectral type estimates of L1.5–L3 and L3–L4.5 for the two components. Published spectroscopy of lithium and gravity-sensitive features gives an estimated age of 0.1–0.8 Gyr, and the resulting model-derived mass estimates are 0.025–0.07 M_{\odot} and 0.02–0.65 M_{\odot} for Kelu-1A and 1B, respectively. Assuming the relation between T_{eff} and spectral type derived for field objects is appropriate for the somewhat younger Kelu-1, the models provide a refined age estimate of 0.3–0.8 Gyr, component masses of 0.05–0.07 M_{\odot} and 0.045–0.065 M_{\odot} , and a mass ratio of about 0.9.

With an estimated orbital period of about 35 yrs (\approx 15–105 yr range), Kelu-1 joins the growing ranks of nearby L dwarf binaries potentially suitable for dynamical mass determinations. Such measurements would be a valuable test of substellar evolutionary models. In addition, there are only six Li-bearing L dwarf binaries known so far, including Kelu-1AB; dynamical masses for these systems would directly test the model-predicted \approx 0.065 M_{\odot} limit for lithium burning. Kelu-1 is one of four known Li-bearing L binaries with projected separations greater than 0.2''. For these systems, determining whether one or both components possess lithium could provide high precision constraints on their ages, via the differences in the lithium depletion timescale of the individual components.

Our Kelu-1 study represents the first LGS AO observations of a brown dwarf. But it provides only a small indication of what will be possible as the Keck LGS system matures and other 8-10-meter class telescopes deploy LGS AO systems. Given the importance of high angular resolution near-IR observations for substellar astronomy, our work is surely only the first of many studies arising from this new capability.

We gratefully acknowledge the Keck LGS AO team for their impressive efforts in bringing the LGS AO system to fruition. It is a pleasure to thank Antonin Bouchez, David LeMignant, Marcos van Dam, Randy Campbell, Gary Punawai, Peter Wizinowich, and the Keck Observatory staff for their assistance with the observations; Adam Burrows and Isabelle Baraffe for providing model calculations; Neill Reid and Mike Cushing for insightful discussions; and John Rayner, Dave Golimowski, and Gibor Basri for comments on the manuscript. Our research has benefitted from the *HST* Archive; the 2MASS data products; the SIMBAD database operated at CDS, Strasbourg, France; and the M, L, and T dwarf compendium housed at DwarfArchives.org and maintained by Chris Gelino, Davy Kirkpatrick, and Adam Burgasser (Kirkpatrick 2003; Gelino et al. 2004). This work has been supported by NSF grant AST-0507833 and the Alfred P. Sloan Foundation. We thank Alan Stockton for a fortuitous swap of observing nights. Finally, the authors wish to recognize and acknowledge the very significant cultural role and reverence that the summit of Mauna Kea has always had within the indigenous Hawaiian community. We are most fortunate to have the opportunity to conduct observations from this mountain.

REFERENCES

- Bailer-Jones, C. A. L. 2002, *A&A*, 389, 963
- Bailer-Jones, C. A. L. & Lamm, M. 2003, *MNRAS*, 339, 477
- Baraffe, I., Chabrier, G., Allard, F., & Hauschildt, P. H. 1998, *A&A*, 337, 403
- Baraffe, I., Chabrier, G., Barman, T. S., Allard, F., & Hauschildt, P. H. 2003, *A&A*, 402, 701
- Basri, G. 1998, in *ASP Conf. Ser.* 134: Brown Dwarfs and Extrasolar Planets, 394
- Basri, G., Marcy, G. W., & Graham, J. R. 1996, *ApJ*, 458, 600
- Basri, G., Martin, E., Ruiz, M. T., Delfosse, X., Forveille, T., Epcstein, N., Allard, F., & Leggett, S. K. 1998, in *ASP Conf. Ser.* 154: Cool Stars, Stellar Systems, and the Sun, 1819
- Basri, G., Mohanty, S., Allard, F., Hauschildt, P. H., Delfosse, X., Martín, E. L., Forveille, T., & Goldman, B. 2000, *ApJ*, 538, 363
- Bate, M. R., Bonnell, I. A., & Bromm, V. 2002, *MNRAS*, 332, L65
- Bessell, M. S. & Brett, J. M. 1988, *PASP*, 100, 1134
- Bouchez, A. H. et al. 2004, in *Advancements in Adaptive Optics*. Edited by Domenico B. Calia, Brent L. Ellerbroek, and Roberto Ragazzoni. *Proceedings of the SPIE*, Vol. 5490, 321–330
- Bouy, H., Brandner, W., Martín, E. L., Delfosse, X., Allard, F., & Basri, G. 2003, *AJ*, 126, 1526
- Bouy, H. et al. 2004, *A&A*, 423, 341
- Brown, R. A. 2004, *ApJ*, 607, 1003
- Burgasser, A. J., Kirkpatrick, J. D., & Lowrance, P. J. 2005, *AJ*, 129, 2849
- Burrows, A., Hubbard, W. B., Lunine, J. I., & Liebert, J. 2001, *Reviews of Modern Physics*, 73, 719
- Burrows, A., Marley, M., Hubbard, W. B., Lunine, J. I., Guillot, T., Saumon, D., Freedman, R., Sudarsky, D., & Sharp, C. 1997, *ApJ*, 491, 856
- Burrows, A. & Sharp, C. M. 1999, *ApJ*, 512, 843
- Chabrier, G., Baraffe, I., & Plez, B. 1996, *ApJ*, 459, L91
- Clarke, F. J., Tinney, C. G., & Covey, K. R. 2002, *MNRAS*, 332, 361
- Clarke, F. J., Tinney, C. G., & Hodgkin, S. T. 2003, *MNRAS*, 341, 239
- Close, L. M., Siegler, N., Freed, M., & Biller, B. 2003, *ApJ*, 587, 407

- Dahn, C. et al. 2000, in ASP Conf. Ser. 212: From Giant Planets to Cool Stars, 74
- Dahn, C. C. et al. 2002, AJ, 124, 1170
- Delfosse, X. et al. 1999, A&AS, 135, 41
- Foy, R. & Labeyrie, A. 1985, A&A, 152, L29
- Freed, M., Close, L. M., & Siegler, N. 2003, ApJ, 584, 453
- Geballe, T. et al. 2002, ApJ, 564, 466
- Gelino, C. R., Kirkpatrick, J. D., & Burgasser, A. J. 2004, BAAS, 205
- Gizis, J. E., Reid, I. N., Knapp, G. R., Liebert, J., Kirkpatrick, J. D., Koerner, D. W., & Burgasser, A. J. 2003, AJ, 125, 3302
- Golimowski, D. A. et al. 2004a, AJ, 127, 3516
- . 2004b, AJ, 128, 1733
- Happer, W., MacDonald, G. J., Max, C. E., & Dyson, F. J. 1994, Optical Society of America Journal A, 11, 263
- Hawley, S. L. et al. 2002, AJ, 123, 3409
- Kirkpatrick, J. D. 2003, in Proceedings of IAU Symposium 211: Brown Dwarfs, ed. E. Martin, 189
- Kirkpatrick, J. D., Reid, I. N., Liebert, J., Cutri, R. M., Nelson, B., Beichman, C. A., Dahn, C. C., Monet, D. G., Gizis, J. E., & Skrutskie, M. F. 1999, ApJ, 519, 802
- Kirkpatrick, J. D., Reid, I. N., Liebert, J., Gizis, J. E., Burgasser, A. J., Monet, D. G., Dahn, C. C., Nelson, B., & Williams, R. J. 2000, AJ, 120, 447
- Knapp, G. R. et al. 2004, AJ, 127, 3553
- Koerner, D. W., Kirkpatrick, J. D., McElwain, M. W., & Bonaventura, N. R. 1999, ApJ, 526, L25
- Lachaume, R., Dominik, C., Lanz, T., & Habing, H. J. 1999, A&A, 348, 897
- Lane, B. F., Zapatero Osorio, M. R., Britton, M. C., Martín, E. L., & Kulkarni, S. R. 2001, ApJ, 560, 390
- Leggett, S. K. et al. 2002, ApJ, 564, 452
- Liu, M. C., Fischer, D. A., Graham, J. R., Lloyd, J. P., Marcy, G. W., & Butler, R. P. 2002, ApJ, 571, 519
- Marley, M. S., Seager, S., Saumon, D., Lodders, K., Ackerman, A. S., Freedman, R. S., & Fan, X. 2002, ApJ, 568, 335

- Martín, E. L., Brandner, W., & Basri, G. 1999a, *Science*, 283, 1718
- Martín, E. L., Delfosse, X., Basri, G., Goldman, B., Forveille, T., & Zapatero Osorio, M. R. 1999b, *AJ*, 118, 2466
- McCaughrean, M. J., Close, L. M., Scholz, R.-D., Lenzen, R., Biller, B., Brandner, W., Hartung, M., & Lodieu, N. 2004, *A&A*, 413, 1029
- McGovern, M. R., Kirkpatrick, J. D., McLean, I. S., Burgasser, A. J., Prato, L., & Lowrance, P. J. 2004, *ApJ*, 600, 1020
- McLean, I. S., McGovern, M. R., Burgasser, A. J., Kirkpatrick, J. D., Prato, L., & Kim, S. S. 2003, *ApJ*, 596, 561
- Metchev, S. A. & Hillenbrand, L. A. 2004, *ApJ*, 617, 1330
- Monet, D. G. et al. 2003, *AJ*, 125, 984
- Potter, D., Martín, E. L., Cushing, M. C., Baudoz, P., Brandner, W., Guyon, O., & Neuhauser, R. 2002, *ApJ*, 567, L133
- Rebolo, R., Martin, E. L., & Magazzu, A. 1992, *ApJ*, 389, L83
- Rebolo, R., Zapatero Osorio, M. R., Madruga, S., Bejar, V. J. S., Arribas, S., & Licandro, J. 1998, *Science*, 282, 1309
- Reid, I. N., Gizis, J. E., Kirkpatrick, J. D., & Koerner, D. W. 2001, *AJ*, 121, 489
- Ruiz, M. T., Leggett, S. K., & Allard, F. 1997, *ApJ*, 491, L107
- Simons, D. A. & Tokunaga, A. 2002, *PASP*, 114, 169
- Stephens, D. C. & Leggett, S. K. 2004, *PASP*, 116, 9
- Thompson, L. A. & Gardner, C. S. 1987, *Nature*, 328, 229
- Tinney, C. G., Delfosse, X., & Forveille, T. 1997, *ApJ*, 490, L95
- Tokunaga, A. T., Simons, D. A., & Vacca, W. D. 2002, *PASP*, 114, 180
- Torres, G. 1999, *PASP*, 111, 169
- Ushomirsky, G., Matzner, C. D., Brown, E. F., Bildsten, L., Hilliard, V. G., & Schroeder, P. C. 1998, *ApJ*, 497, 253
- Vrba, F. J. et al. 2004, *AJ*, 127, 2948
- Wizinowich, P. L. et al. 2004, in *Advancements in Adaptive Optics*. Edited by Domenico B. Calia, Brent L. Ellerbroek, and Roberto Ragazzoni. Proceedings of the SPIE., Vol. 5490, 1–11

Zapatero Osorio, M. R., Lane, B. F., Pavlenko, Y., Martín, E. L., Britton, M., & Kulkarni, S. R.
2004, ApJ, 615, 958

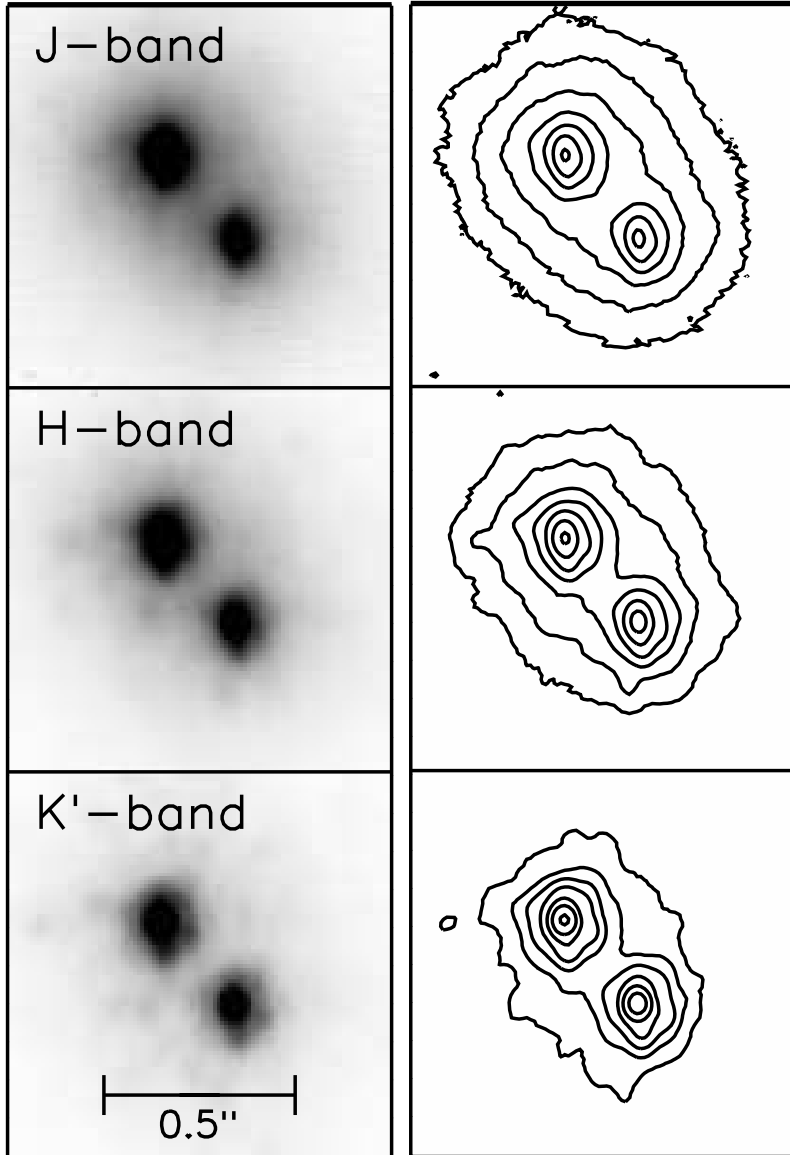


Fig. 1.— JHK' -band imaging of Kelu-1 from Keck LGS AO. North is up and east is left. Each image is $1.0''$ (18.7 AU) on a side. The binary separation is $0.291'' \pm 0.002''$ with a position angle of $221.2^\circ \pm 0.6^\circ$ east of north. The contours are drawn from 90.0, 45.0, 22.5, 11.2, 5.6, 2.8, and 1.4% of the peak value in each bandpass. The central region of the PSF is slightly elongated in the vertical direction due to the combined effects of atmospheric dispersion (more apparent at the shorter wavelengths) and slight asymmetries in the first Airy ring (more apparent at the longer wavelengths).

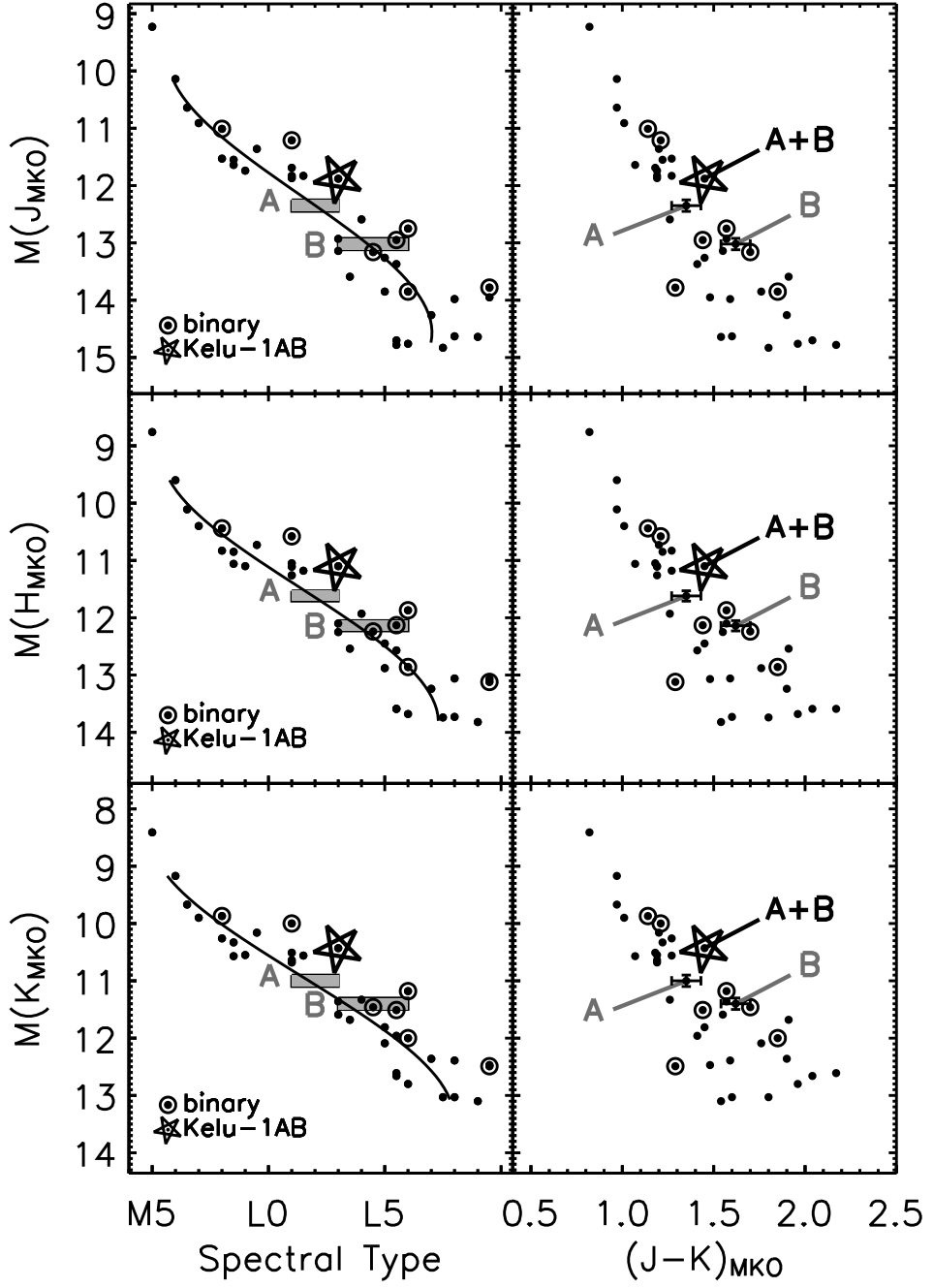


Fig. 2.— Near-IR properties of Kelu-1A and B compared with nearby late-M dwarfs and L dwarfs (see § 3). Integrated-light data for known binaries are shown as ringed dots, with Kelu-1AB shown as a star. **Left:** JHK absolute magnitudes versus spectral types on the Geballe et al. (2002) system. The observational constraints from the absolute magnitudes and the spectral type range inferred from JHK colors, flux ratios, and integrated-light spectra are shown as shaded boxes. The solid lines are fits to the spectral type as a function of absolute magnitude for the nearby dwarfs, excluding known binaries. The final inferred spectral types are L1.5–L3 for Kelu-1A and L3–L4.5 for Kelu-1B. **Right:** Infrared color-magnitude diagrams. In integrated light, Kelu-1AB appears to be unusually red for its absolute magnitude. However, the resolved properties of the two components (shown as dots with error bars) are consistent with other apparently single L dwarfs.

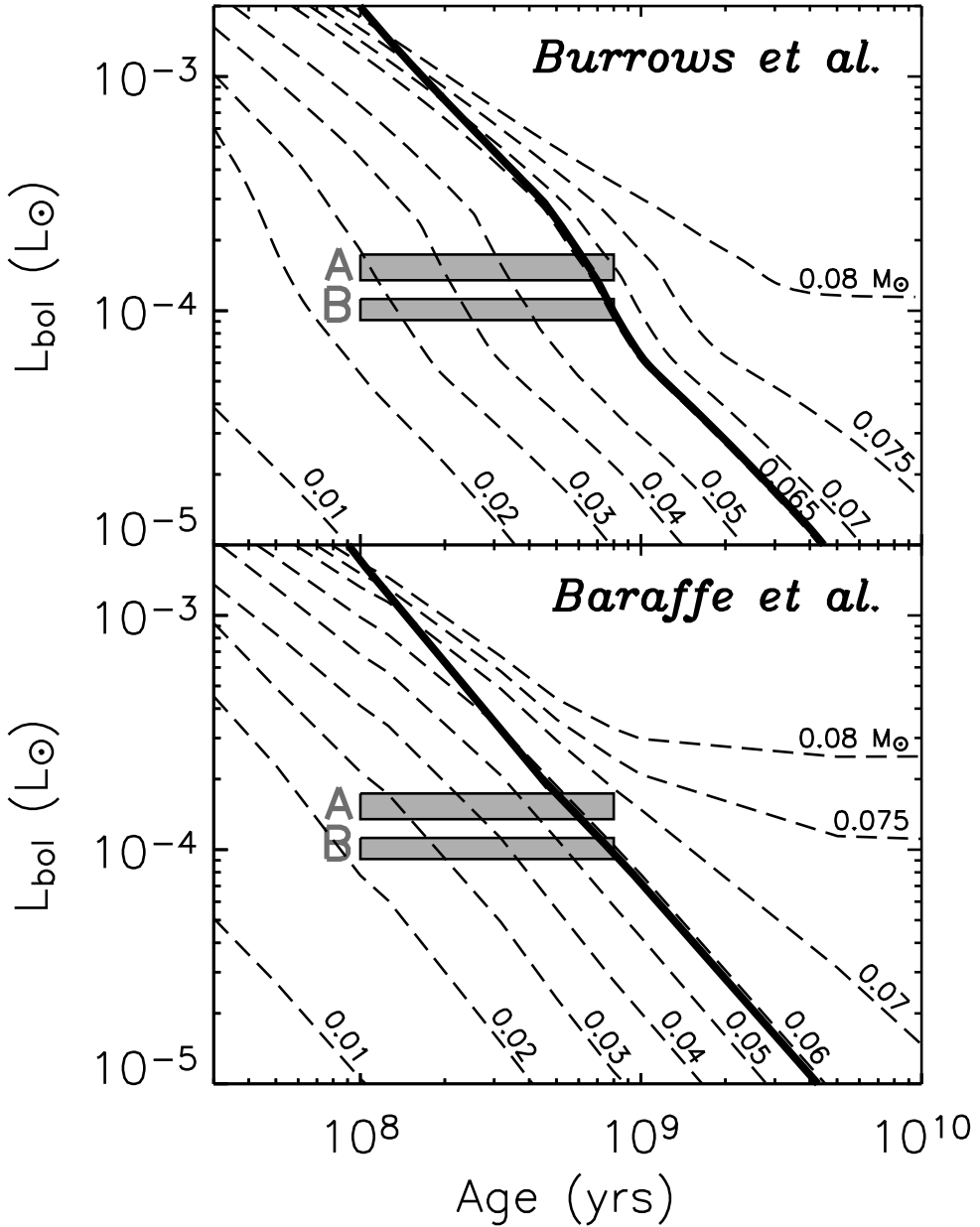


Fig. 3.— Mass estimates for Kelu-1A and 1B derived from components' inferred L_{bol} and age, using Burrows et al. (1997) and Baraffe et al. (1998, 2003) models. The stellar/substellar boundaries for the two sets of models are at $\approx 0.075 M_{\odot}$ and $\approx 0.072 M_{\odot}$, respectively. Dashed lines show models of constant mass, labeled in units of M_{\odot} . The heavy solid line represents the 1% lithium depletion boundary; objects to the right of the line have depleted their lithium. The shaded rectangles show the observational constraints for Kelu-1A and 1B. The estimated age range is 0.1–0.8 Gyr, based on optical spectroscopy (see § 4). Using the Burrows models, the resulting mass estimates are 0.03 – $0.07 M_{\odot}$ and 0.025 – $0.065 M_{\odot}$ for components A and B, respectively. The Baraffe models predict masses of 0.025 – 0.07 and 0.02 – $0.06 M_{\odot}$. Since the iso-mass lines are mostly vertical in this plot, the uncertainties in the masses are dominated by the uncertain age of the system.

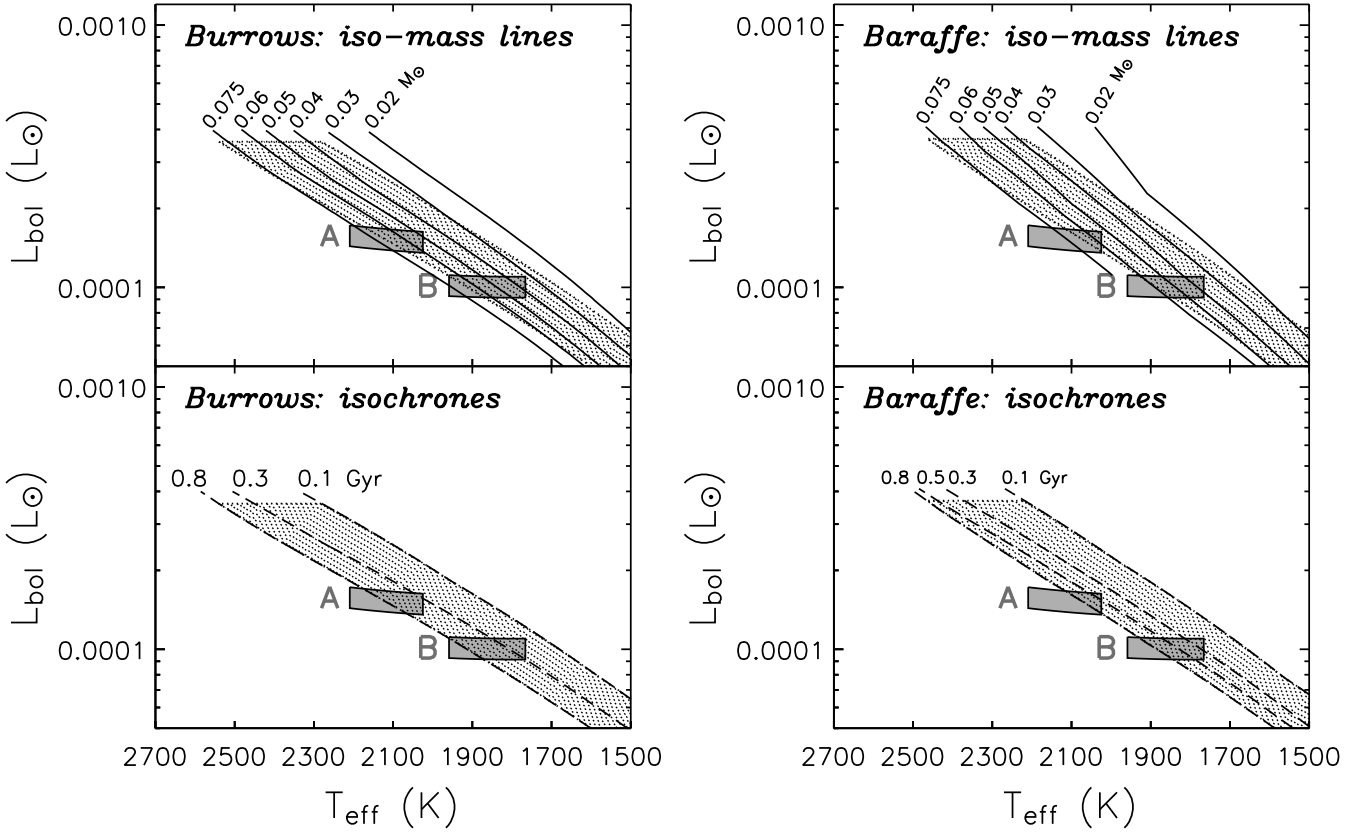


Fig. 4.— Refined mass estimates for Kelu-1A and 1B, based on the estimated T_{eff} 's combined with the constraints in Figure 3 (see § 4.3). The dark shaded horizontal regions show the T_{eff} and L_{bol} range of the two components. (Note that the Golimowski et al. 2004a bolometric corrections depend on the spectral type, and hence the $\{T_{\text{eff}}, L_{\text{bol}}\}$ constraints are curved regions rather than rectangles.) The dotted region shows the estimated age range of 0.1–0.8 Gyr (truncated at the high luminosity end for plotting purposes). Thus, the intersection of the dotted and the shaded regions represents all the available observational constraints. **Top plots:** Model tracks of constant mass are overplotted. The inferred upper mass estimates are 0.07 and 0.065 M_{\odot} for A and B, respectively, from the Burrows models. The Baraffe models give values of 0.07 and 0.06 M_{\odot} . **Bottom plots:** Same data and models, now with only model isochrones overplotted for clarity. (The isochrones in fact are nearly parallel to the iso-mass lines.) The observed $\{T_{\text{eff}}, L_{\text{bol}}\}$ of Kelu-1A suggest that a lower age limit of ≈ 0.3 –0.4 Gyr, depending on the choice of models. This leads to lower mass estimates of 0.05 and 0.045 M_{\odot} for the two components.

Table 1. Keck LGS AO Results^a

Property	Measurement
a (mas)	291 ± 2
ϕ (deg)	221.2 ± 0.6
ΔJ (mags)	0.67 ± 0.04
ΔH (mags)	0.52 ± 0.03
$\Delta K'$ (mags)	0.40 ± 0.02

^aAll photometry on the MKO system.

Table 2. Resolved Properties of Kelu-1^a

Property	Kelu-1A	Kelu-1B
J (mags)	13.70 ± 0.06	14.37 ± 0.06
H (mags)	12.97 ± 0.05	13.49 ± 0.05
K (mags)	12.35 ± 0.06	12.75 ± 0.06
$J - H$ (mags)	0.73 ± 0.08	0.88 ± 0.08
$H - K$ (mags)	0.62 ± 0.08	0.74 ± 0.08
$J - K$ (mags)	1.35 ± 0.08	1.62 ± 0.08
$M(J)$ (mags)	12.35 ± 0.10	13.02 ± 0.10
$M(H)$ (mags)	11.62 ± 0.09	12.14 ± 0.09
$M(K)$ (mags)	11.00 ± 0.10	11.40 ± 0.10
Estimated spectral type	L1.5 – L3	L3 – L4.5
$\log(L_{bol}/L_\odot)$	–3.76 to –3.87	–3.95 to –4.04

^aAll photometry on the MKO photometric system.